An Event in Water Exchange between Continental Shelf and the Kuroshio off Southern Japan: Lagrangian Tracking of a Low-Salinity Water Mass on the Kuroshio

NORIHISA IMASATO AND BO QIU

Geophysical Institute, Kyoto University, Kyoto, Japan

(Manuscript received 28 October 1985, in final form 9 January 1987)

ABSTRACT

Low-salinity water masses were occasionally observed in spring and summer on the surface of the Kuroshio, south of Japan. Many of the masses were accompanied by excessive discharges of fresh water from major rivers in southern Japan and were observed 20–40 days after the discharges. The salinity difference between the low-salinity water mass and the Kuroshio was closely proportional to the river water discharge.

To specify their origin, the behavior of a water mass seen on 10 August 1979 was studied in detail. A large number of labeled particles were deployed in the water mass and were tracked numerically by the Euler–Lagrangian method. The fresh water forming the low-salinity water mass in the Kuroshio was concluded to originate in the Seto-Inland Sea and the Tosa Bay, and 58% of the river water discharge was sufficient to form the low-salinity water mass. When a particle in the Kuroshio flows along the southern coast of Japan, it receives coastal water which is discharged in excess due to snow melting in spring and heavy rainfall such as that caused by a stagnating front, a cyclone or a typhoon. The parcel of coastal water is estimated to move from the river mouth to the continental shelf region at a mean speed of 5–10 cm s^{-1}.

1. Introduction

The Seto-Inland Sea of Japan (Fig. 1) stores a large amount of fresh water discharged from a number of rivers. After passing through the Kii or the Bungo Channel, the discharged fresh water spreads on the continental shelf area to meet the warm and high-salinity offshore water of the Kuroshio to make a sharp Kuroshio front. According to Kawabe (1985), the current path of the Kuroshio offshore of Japan is classified into three types, i.e., (i) nearshore non-large-meander path, (ii) offshore non-large-meander path and (iii) large-meander path (Fig. 2a). These paths are along the continental shelf edge offshore of southern Japan. Figure 2b shows the distribution at the sea surface of salinity (solid curve) and dynamic depth anomaly ΔD referred to 1000 db (broken curve), which demonstrates a representative state associated with the offshore non-large-meander path of the Kuroshio. The coastal water with a salinity of less than 34.0‰ is distributed on the shelf region of the onshore side of the Kuroshio, and water with a relatively high salinity is distributed on the Kuroshio and its offshore side. The isohaline curve is parallel with the contour curve of the dynamic depth anomaly, and a large gradient of salinity, the so-called Kuroshio haline front, is found between the Kuroshio and shelf region.

Kuroda (1969) observed relatively low-salinity waters with a large diatom population in the surface layer on the offshore side of the Kuroshio, and speculated that the waters originated from the coast. Takano et al. (1981), on the other hand, observed remarkably low-

salinity waters on the coastal side of the Kuroshio front. The salinity of the waters was found to be 0.4‰ lower than that of the surrounding waters, but no temperature difference was discerned. They also detected a low-salinity water mass on the offshore side of the front. The existence of such low-salinity water masses suggests that water mass exchange takes place across the Kuroshio front.

Similar phenomena have also been recognized in the Gulf Stream region. Ford et al. (1952) found a remarkable cold low-salinity water mass extending discontinuously on the shelf side of the Gulf Stream. Ford and Miller (1952) surmised that the water originated in the Middle Atlantic Bight. Using an airborne radiation thermometer, Fisher (1972) described the entrainment of shelf water by the Gulf Stream system northeast of Cape Hatteras and estimated the seaward transport to be of the magnitude of 10^4 m^3 s^{-1}. Kupferman and Garfield (1977), using hydrodynamic and drogue measurements to study the entrainment, also estimated the mean transport of the shelf water across the shelf water–Gulf Stream boundary to be 10^4 m^3 s^{-1}.

Besides the exchange process of entrainment, Horne (1978) considered horizontal mixing through an interleaving process and vertical mixing through double diffusion. Lambert (1982) also studied two mechanisms of cross-stream exchange, cross-front interleaving and surface intrusion of the Gulf Stream into the shelf water. The former was proposed as a result of cross-stream cellular circulation due to curvature of the Gulf Stream. Using both satellite pictures and field observation data, the role on water exchange played by warm-core rings
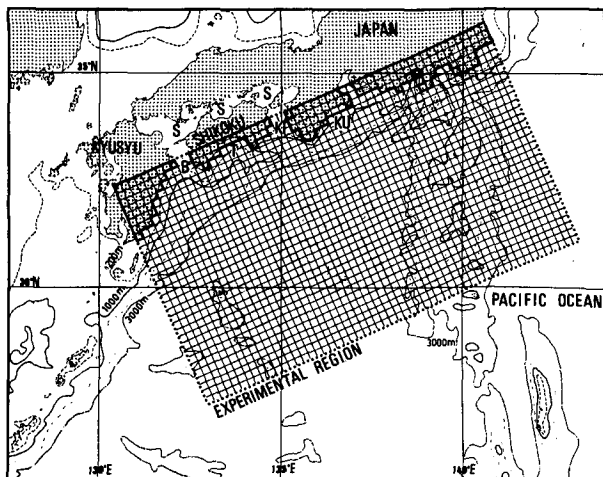
FIG. 1. Experimental region. Dotted line denotes the open boundary. S, B, T, KI and KU denote the Seto-Inland Sea, the Bungo Channel, the Tosa Bay, the Kii Channel and the Kumanonada, respectively.

and cold-core rings produced at boundaries of the Gulf Stream has also been intensively investigated (e.g., Saunders, 1971; Fuglister, 1972; Lee et al., 1981).

While examining the oceanographic data which had been taken in the numerical experimental region shown in Fig. 1, we found a large water mass of low-salinity appearing occasionally on the current axis of the Kuroshio. Figure 3 shows a representative example. The distributions shown in panels A and B are based on the data obtained from April to June 1979 and those in panels C, D and E on the data obtained from July to September 1979. Panels A and C of Fig. 3 show the distribution at the sea surface of dynamic depth anomaly ΔD referred to 1000 db, and panels B and D show the distribution of salinity in the surface layer. Panel B contains no distinctive low-salinity water mass, but panel D contains a large low-salinity water mass on the Kuroshio around 137°E and 32°N. Panel E shows the vertical profile of salinity along the survey line across the low-salinity water mass. This figure demonstrates that during July to September 1979, the low-salinity water is confined within the surface layer shallower than 40 m.

We speculated that the average distribution of salinity in the coastal and shelf regions is maintained by the river waters of annual mean volume and that a discharge exceeding this volume produces a low-salinity water mass. Therefore, the study of such low-salinity water masses reveals the type of water exchange between the coastal water and more saline offshore water along the continental shelf off southern Japan. In this study, we used the Euler-Lagrangian method of tracking numerically a number of labeled particles (Imasato et al., 1980; Awaji et al., 1980) to investigate what and where the origin of the low-salinity water mass on the

Kuroshio is, what the physical process of water exchange between the shelf water and the offshore saline water of the Kuroshio across the Kuroshio-front is, and also how fluctuation of the meandering path of the Kuroshio affects the water exchange between these two kinds of waters.

2. Data analysis

We examined the distributions of dynamic depth anomaly, salinity and water temperature in the surface layer obtained by the serial observations of all cruises which the Maritime Safety Agency (Oceanographic Summarized Report, 1967–1981) and the Kobe Marine Observatory of Japan (Oceanographic Prompt Report, 1967–1981) carried out during the past 15 years in the Kuroshio region near Japan (experimental region in Fig. 1). We found that the low-salinity water masses such as those shown in Fig. 3d appeared on the current axis of the Kuroshio 13 times in summer (40% of all the summer cruises) and nine times in May (35%), but not in autumn or winter. This situation is well shown in Fig. 4, where open squares denote a cruise encountering a low-salinity water mass on the current axis of the Kuroshio, and solid circles denote a cruise which did not encounter a low-salinity water mass. This seasonal appearance suggests that the low-salinity water masses are related to a heavy rain fall caused by snow melting in spring and a stagnating front, a cyclone or a typhoon.

Figure 5a shows the relationship between the appearance of the low-salinity water and that of the heavy discharge of fresh water from rivers along the coast of the Seto Inland Sea, the Bungo Channel, the Kii Channel and the Tosa Bay (Fig. 1). Here, a total discharge five times larger than the annual-mean value will be regarded as a "heavy discharge". In this figure, open squares and half-solid squares show the time when the low-salinity water mass was encountered, and the vertical solid arrowheads show the time when a heavy discharge of river water occurred. Therefore, the arrow shows the time-lag between the appearance of a low-salinity water mass, and the last heavy discharge of river water. Figure 5a shows that the 15 cases indicated by the symbol open squares are accompanied by a heavy discharge from the major rivers, and the seven cases indicated by the half solid squares are not related to any heavy discharge. The latter cases are concentrated in May, for an unknown reason. Figure 5b shows a histogram of the time lags, which are indicated by the arrows in Fig. 5a and suggest that the low-salinity water masses were mainly observed 20–40 days after the last heavy discharge from the major rivers in southern Japan.

The numeral on the right of the open and half solid squares in Fig. 5a denote the observed salinity difference (ΔS) between the low-salinity water mass and the adjacent sea water in the Kuroshio, and shows that the
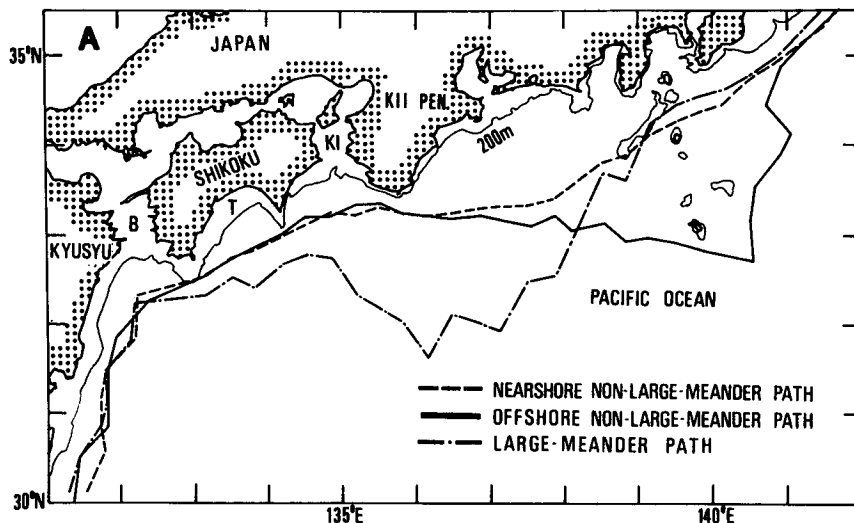
FIG. 2a. Three representative curve paths of the Kuroshio south of Japan. Dashed line: nearshore non-large-meander path, solid line: offshore non-large-meander path and dash-dot line: large-meander path (after Kawabe, 1985). B, T and KI: the same as in Fig. 1.

low-salinity water mass has a tendency to take a smaller value of salinity difference ΔS in spring and a larger value in summer. This situation is shown more clearly in the histogram of Fig. 5c, where a white unshaded bar and a shaded bar denote the frequency of a low-salinity water mass being observed in spring and in
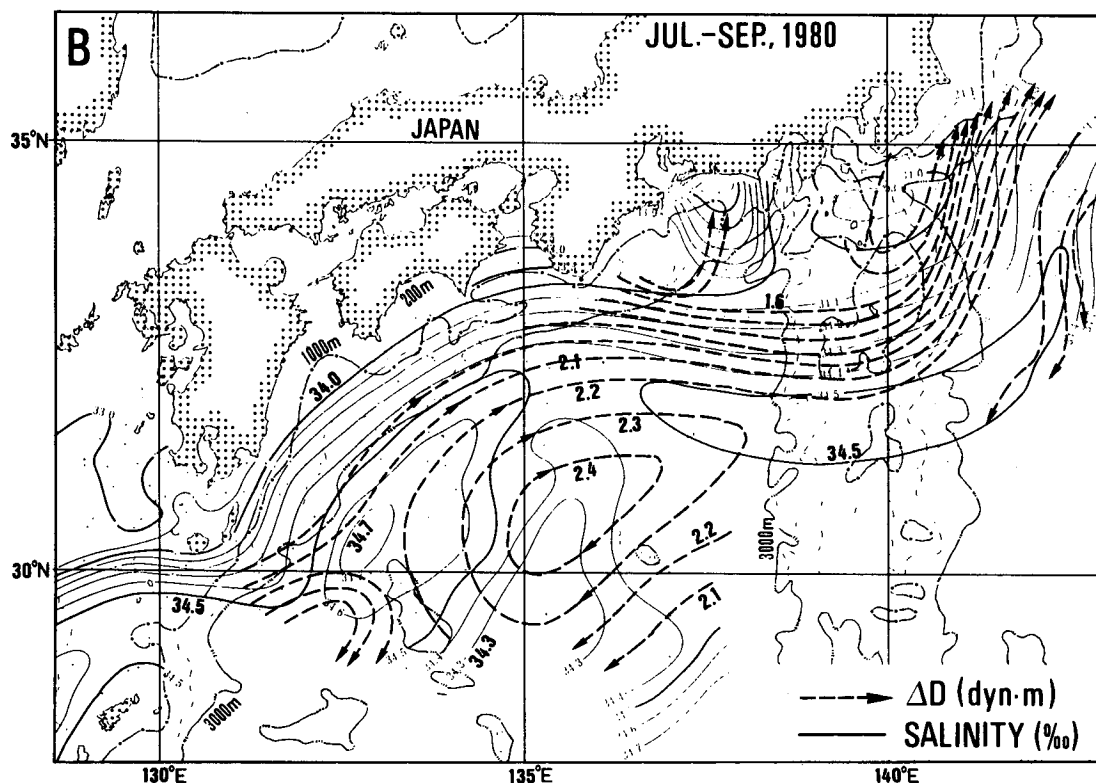

FIG. 2b. Representative salinity distribution associated with the Kuroshio in its offshore non-large-meander path. This distribution is given as a mean state for three months from July to September 1980. The broken line denotes an isoline of the dynamic depth anomaly with the interval of 0.1 dyn m and a solid line denotes the isohaline curve at the interval of 0.1‰.
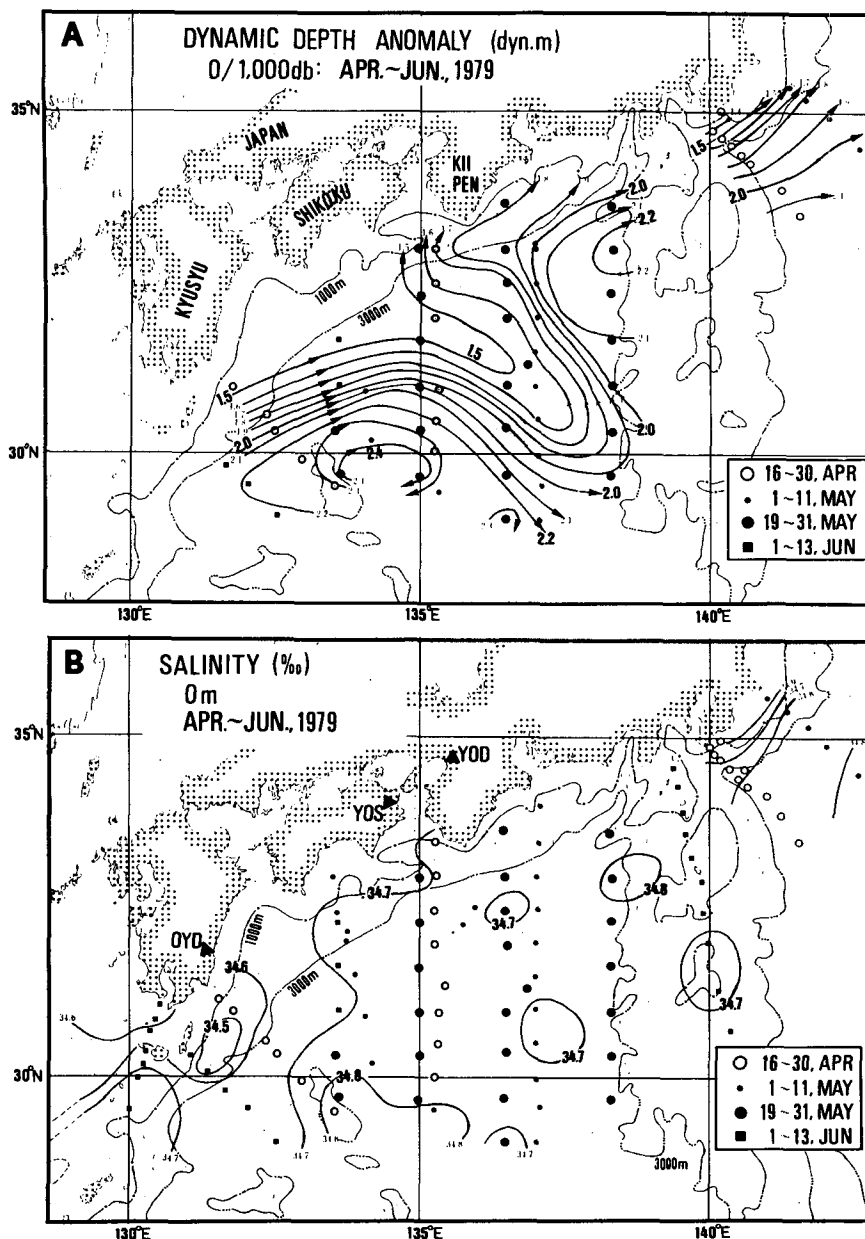
FIG. 3. Distribution of dynamic depth anomaly (dyn m) referred to 1000 db and salinity (‰) at sea surface. Observation points are shown by four kinds of symbols. In panels B and D, the vertical solid arrowheads show the position of the river mouth, and OYD, YOS and YOD denotes the Oyodo, the Yoshino and the Yodo Rivers, respectively. (a) Dynamic depth anomaly ΔD (dyn m), April–June 1979. (b) Salinity (‰), April–June 1979. (c) Dynamic depth anomaly ΔD (dyn m), July–September 1979. (d) Salinity (‰), July–September 1979. (e) Vertical profile of salinity of the low-salinity water mass shown in Fig. 3d.

summer, respectively. The mean value of the observed ΔS was 0.28‰ in spring and 0.55‰ in summer.

Figure 6 shows the relationship between ΔS and the rate of discharged volume of river water, where solid circles correspond to a water mass found on the Kuroshio between 134° and 139°E and open circles correspond to a water mass found east of 139°E. In this

figure, the rate of the discharged volume is given as the mean of the fresh water volume discharged from three major rivers in western Japan (i.e., the Yodo, the Yoshino and the Oyodo Rivers shown in Figs. 3b and 3d), because here we are considering only the coastal water originating from the Seto Inland Sea and the Tosa Bay. Although the fresh water masses denoted by
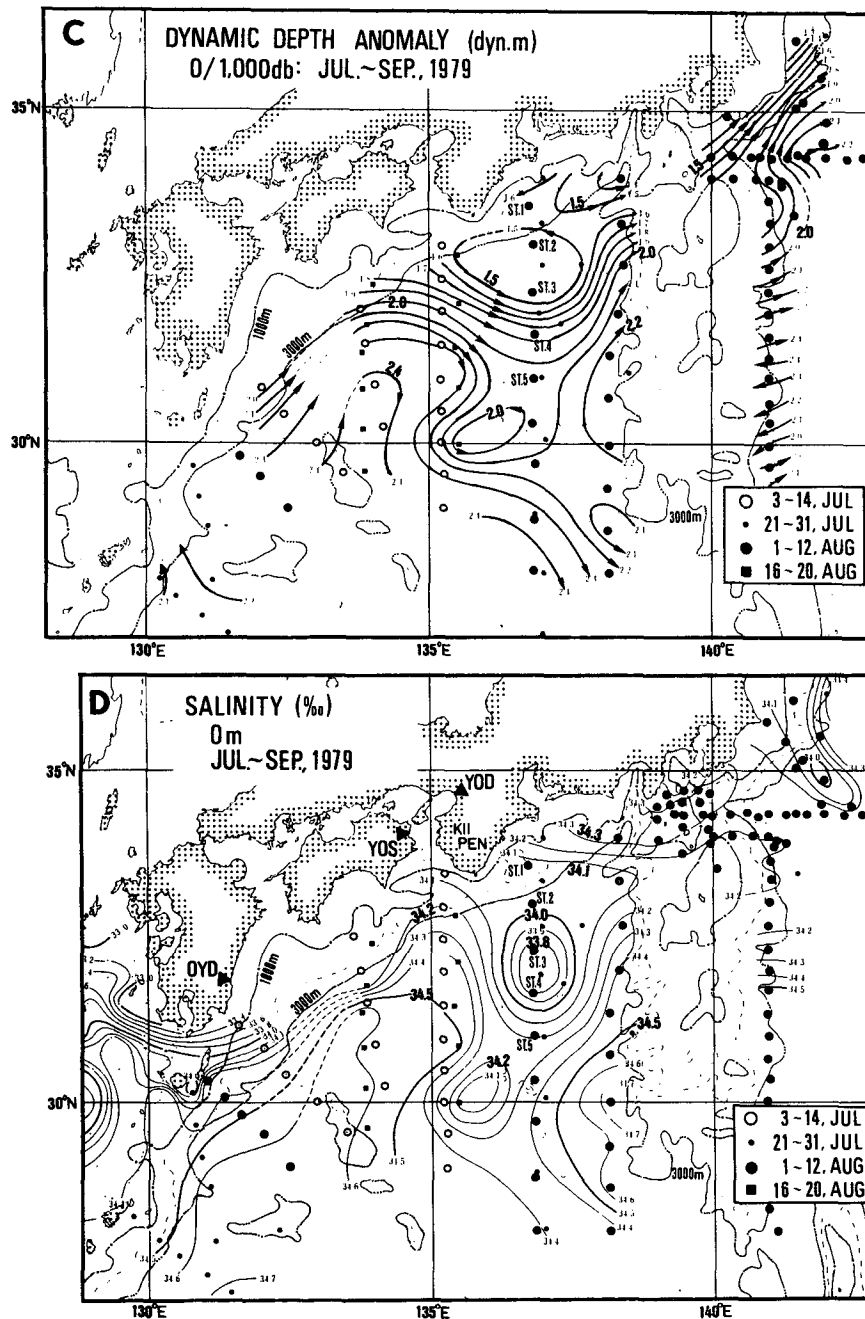
FIG. 3. (*Continued*)

an open circle may originate from the Seto Inland Sea and the Tosa Bay, they are excluded from the present consideration because they have moved too long a distance to have kept their original ΔS values. If open circle water masses are excluded, there is an approximately linear relationship between ΔS and the volume of discharged river water for the data denoted by solid circles. This implies that the emergence of the low-salinity water mass on the Kuroshio was related to an event of "heavy discharge" of river water in the Seto Inland Sea and the Tosa Bay region.

We could not specify the origin of seven low-salinity water masses that appeared on the Kuroshio that were not accompanied by any heavy discharge from rivers along the southern coast of Japan. The masses may have been produced by a sudden and heavy supply
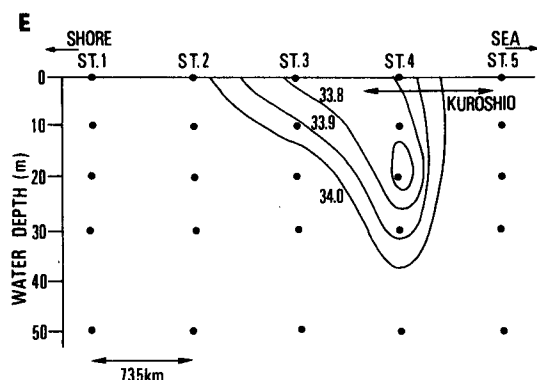
FIG. 3. (*Continued*)

of fresh water such as rain fall on the Kuroshio, or may have originated upstream, such as in the East China Sea.

In the example of a low-salinity water mass on the Kuroshio shown in Fig. 3, the Kuroshio changed from the large-meander state to the offshore non-large-meander one (terminology after Kawabe, 1985). We also examined other cases about the relationship between the emergence of the low-salinity water masses and the meandering of the Kuroshio. No clear connection of the two was found.

3. Origin of low-salinity water on the Kuroshio

a. Numerical tracking of labeled particles

As a representative example, we examined the origin of the low-salinity water mass found on the Kuroshio on 10 August 1979 by the Marine Safety Agency of

Japan (Fig. 3d). We tracked numerically a number of labeled particles deployed in the experimental region enclosed by the heavy solid and dotted lines shown in Fig. 1, which is 1000 km × 600 km in size and is divided into square meshes of 55 × 32, with a grid size of 19 km. We used the Euler–Lagrangian method (Imasato et al., 1980; Awaji et al., 1980) to track numerically a material particle or a water parcel. In the Euler–Lagrangian method, we can consider a particle which is at the position $\mathbf{X}^0$ at time t, and we can predict a new position of the particle at time $t + \Delta t$ by using Eq. 1:

$$\mathbf{X}_k(t - \Delta t) = \mathbf{X}_k^0(t) + \int_t^{t+\Delta t} \{\mathbf{U}(\mathbf{X}_k^0, t')$$

$$+ \int_t^{t'} \mathbf{U}(\mathbf{X}_k^0, t'')dt'' \cdot \nabla_H \mathbf{U}(\mathbf{X}_k^0, t')\}dt', \quad (1)$$

where suffix k is given to a variable of the kth particle, t is the time, Δt (five hours in this study) is the time interval to calculate the new position of a particle and $\mathbf{U}(\mathbf{X}, t)$ is an Eulerian velocity vector at position $\mathbf{X}$ and time t. Therefore, to track a particle in the region, we need first to obtain the time series of Eulerian velocity fields at successive time interval Δt. However, we have only two sets of data for the three-dimensional distribution of ΔD obtained from the serial observations to a depth of 3500 m (cf. Figs. 3a and 3c).

Judging from the distributions of the observation points in the two observation periods shown in Figs. 3a, b and 3c, d, we assume that each of these distributions represents a three-month mean state, and refer to these two sets of data hereafter as the distributions on 10 May and 10 August 1979. We first assigned spatially the observed ΔD to all grid points to make two
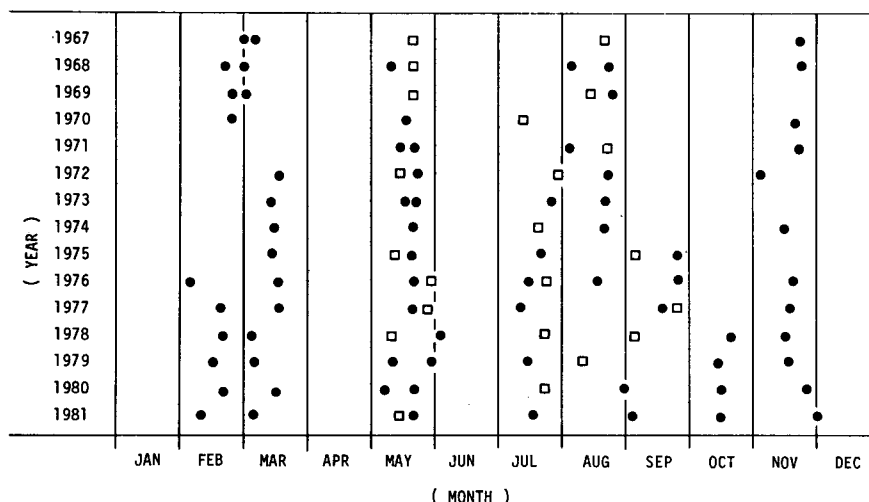

FIG. 4. Seasonal variation in the emergence of a low-salinity water mass. Open squares and solid circles denote a cruise of serial observations in which a low-salinity water mass emerged or did not emerge on the Kuroshio, respectively.
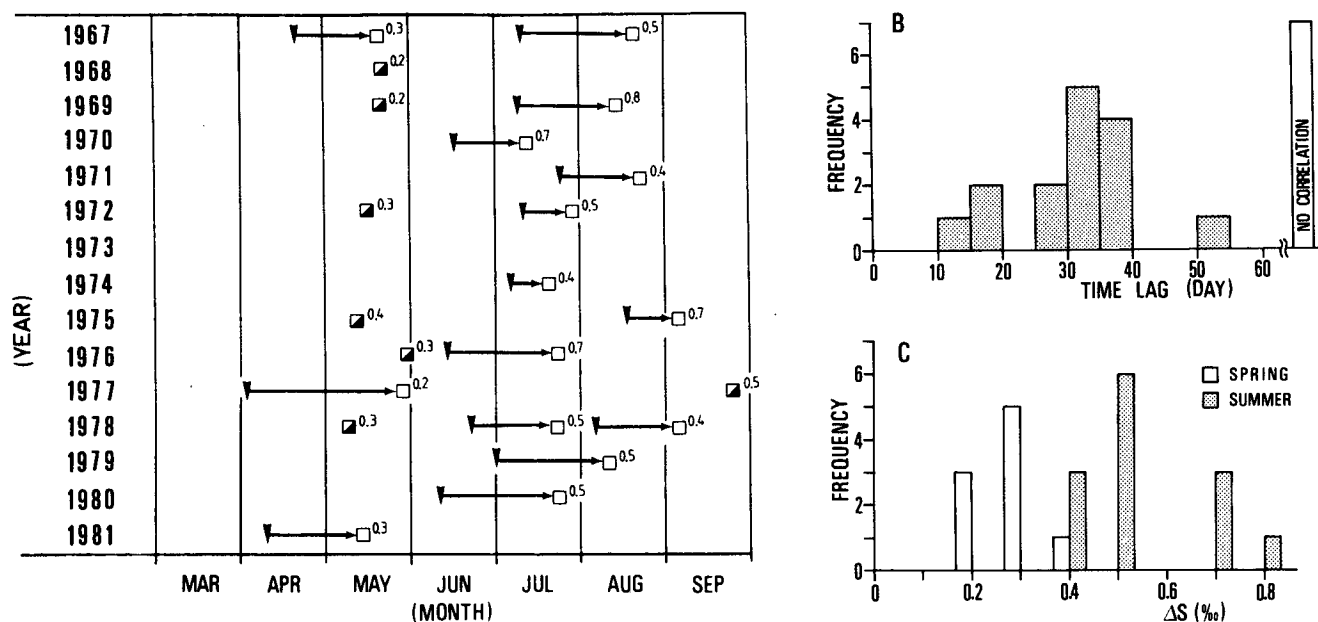
FIG. 5. (a) Relationship between the emergence of the low-salinity water mass (open squares and half-solid squares) and a heavy discharge of river water (solid arrowheads). (b) Histogram of time lag between an observation of a low-salinity water mass on the Kuroshio and the last heavy discharge of river water. (c) Histogram of salinity difference ΔS (‰) between the low-salinity water and adjacent water.

new sets of data on 10 May and 10 August 1979. Then, using these new data sets, we interpolated ΔD linearly in time from 10 May to 10 August 1979 at the interval of $\Delta t = 5$ hours at each grid point. Based on the geostrophic relation, we converted the above time series of the ΔD-field into a time series of Eulerian velocity fields, i.e., $U(X, t)$ in Eq. (1).

Figures 3c and 3d show a characteristic water mass appearing off the Kii Peninsula with salinity less than 34.0‰, lower than that of the adjacent shelf water. Also, half of the low-salinity water mass emerged inside the Kuroshio and the other half inside a large cyclonic

eddylike current adjacent to the meandering Kuroshio. Here the Kuroshio is defined as the region between the isolines of ΔD of 1.6 and 2.0 dyn m, because the observed 20°C isotherm at 200 m below the surface, which has been considered to denote the current axis of the Kuroshio (Kawai, 1969), was situated at the center of these two contour curves. Figure 3 also shows that the Kuroshio in summer, 1979, was in a transient state from a large-meander state to an offshore non-large-meander state and that it approached the coasts of Kyushu and Shikoku closely.

Using the Euler–Lagrangian method described by Eq. (1), we tracked a number of labeled particles to examine the origin of the low-salinity water mass. We examined two hypotheses for the water mass. One is that the water particles moving through the experimental region shown in Fig. 1 do not change in their properties; i.e., the salinity of the water particles is conserved and is predetermined somewhere upstream of Kyushu. The other is that the water particles change in their salinity by receiving coastal waters while moving along the coastal area.

To test the first hypothesis, we released 20 labeled particles (two in each box) on the S-line of asterisks (Fig. 7a) every 20 hours, and tracked them until they reached the eastern or the southern boundary. Figure 7 gives the distributions of the particles at several time points. If the Kuroshio may be assumed to be geostrophic, a particle will be confined to flow on an isoline of ΔD. In this study, where the geostrophic balance is assumed, the water particle moving in (near) the Ku-
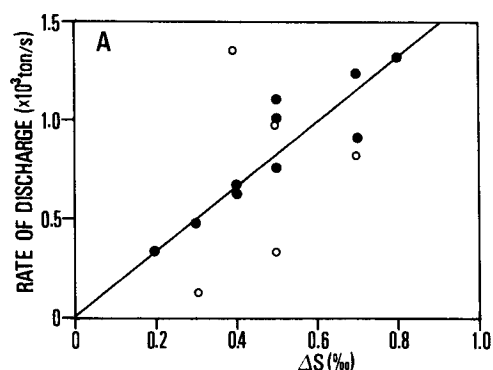

FIG. 6. Relation between salinity difference ΔS (‰) and the rate of river water discharge ($\times 10^3$ ton s^{-1}). Solid circles: water mass observed on the Kuroshio between 134° and 139°E, and open circle: eastward of 139°E.
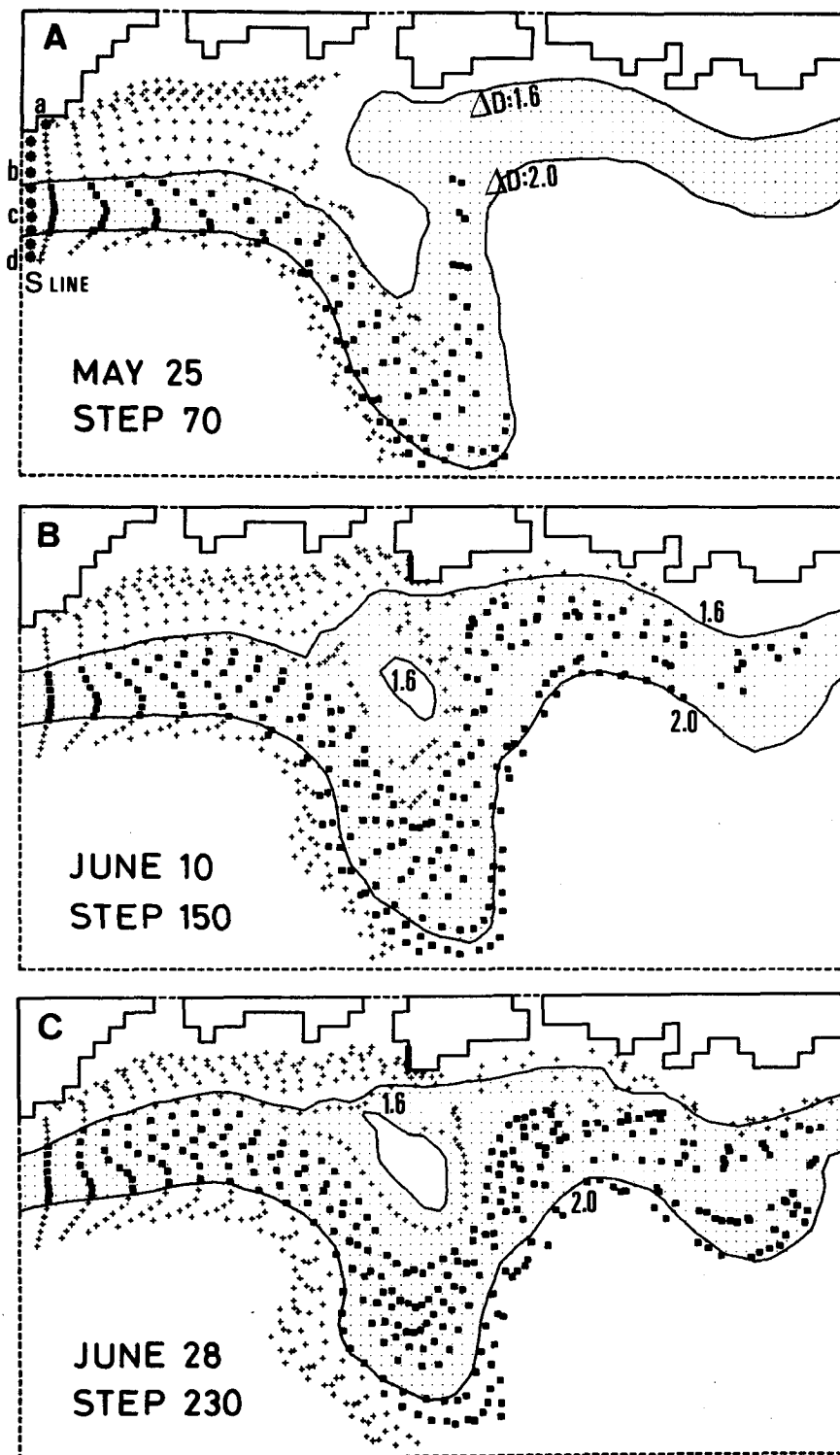
FIG. 7. Results of tracking of labeled particles. Twenty particles were released from the S-line every five hours. Solid squares and crosses show a particle initially released inside and outside the Kuroshio, respectively. Shaded area between two isolines of ΔD of 1.6 and 2.0 dyn m denotes the Kuroshio.

D

JULY 15
STEP 310

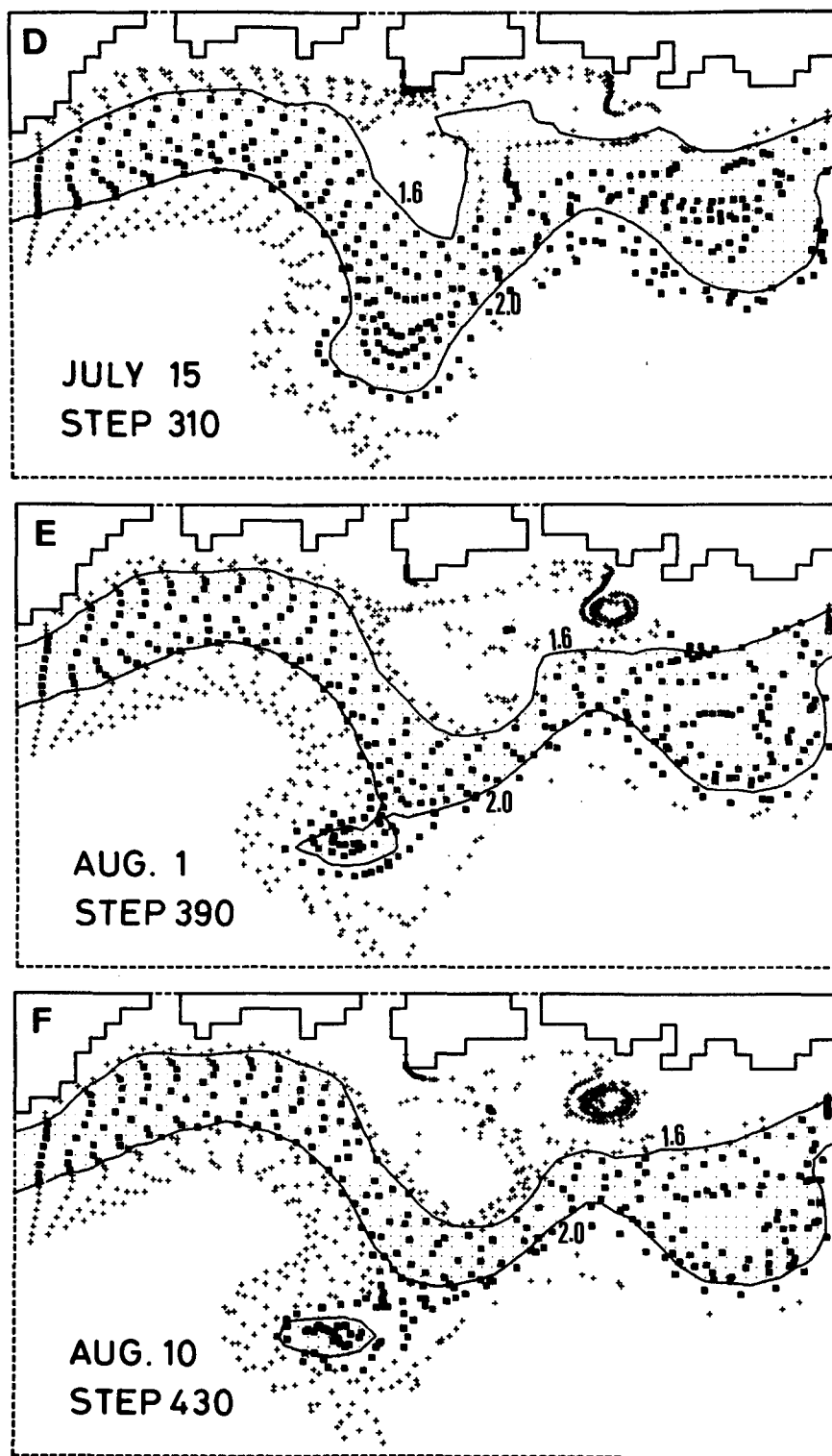E

AUG. 1
STEP 390

F

AUG. 10
STEP 430

FIG. 7. (Continued)

roshio has a chance to come out of (into) the Kuroshio only when the current axis of the Kuroshio fluctuates temporally from the distribution of Fig. 3a to that of Fig. 3c. Figure 7 shows that a few particles crossed the Kuroshio described by two isolines of ΔD of 1.6 and 2.0 dyn m as a result of a slower fluctuation of the

current axis of the Kuroshio compared with the speed of the individual particles. This result suggests that the temporal fluctuation of the current axis of the Kuroshio is not enough to explain the formation of the low-salinity water mass on the Kuroshio.

We determined the time change of salinity that should occur on the S-line (Fig. 7a) to produce the salinity distribution given in Fig. 3d. Relating Fig. 7f with Fig. 3d, the observed salinity was assigned to each particle, which was then caused to follow the reverse course; that is, the course from 10 August 1979 towards 10 May. The particles which were out of the computational domain at the time of 10 August were excluded from the present examination. We detected which particle came back to a grid box on the S-line at time t, what salinity the particle brought back, and obtained a salinity in the grid box at time t by averaging over the particles existing in the grid box at time t. Figure 8 shows the time variation of salinity in each grid box on the S-line from 21 June to 10 August 1979. In this figure, an arrow drawn around 29 July indicates the "return" of the particles which were in the low-salinity water mass on 10 August 1979. If the salinity on the S-line changed as shown in Fig. 8, the observed salinity distribution of Fig. 3d would be produced on 10 August, because we have assumed in the first hypothesis that a water particle in the Kuroshio does not receive any fresh water during its movement along the coast of southern Japan; i.e., we must search for the source somewhere to the west of the S-line. As this study is concerned with the coastal water from the Seto-Inland Sea and the Tosa Bay, let us examine the second hypothesis in the following section.

b. Volume of fresh water in the low-salinity water mass

We assumed that the salinity on the S-line (Fig. 7a) was constant in time, and that each grid box had a salinity value given by the broken line in Fig. 8, which was the maximum value in the grid box. By releasing particles with this assumed salinity and tracking them numerically up to 10 August, we obtained a salinity distribution governed entirely by the Kuroshio system. However, this distribution differed from the observed one shown in Fig. 3d. Their difference (ΔS) was calculated in Fig. 9, which showed that an area with a ΔS as large as 0.7‰ appears at an offshore region of the Kii Peninsula and corresponds to the area of the low-salinity water mass (Fig. 3d).

A ΔS with a large value indicates that a water particle obtained a large amount of fresh water during its movement along the coast of southern Japan. As we are concerned with the origin of the low-salinity water on the Kuroshio, we must necessarily examine the history of the water mass in the area of large ΔS. We deployed labeled particles (four particles in each grid box) in the surface layer with a value of ΔS larger than 0.3‰ (shaded area in Fig. 9), and tracked them as we
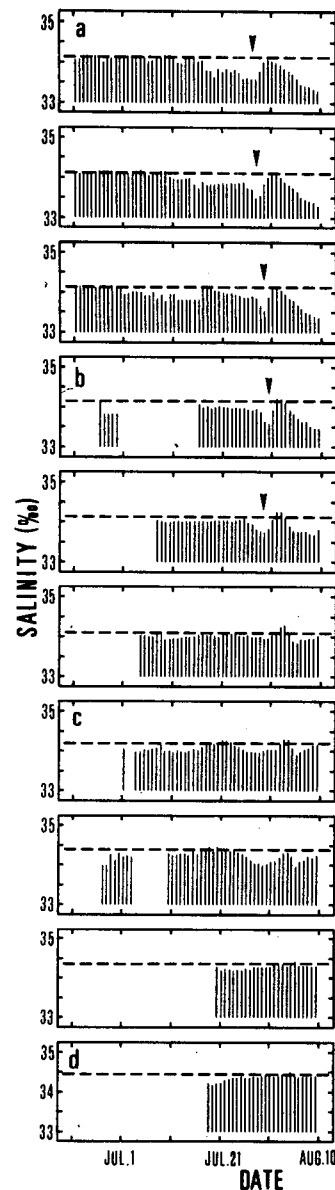

FIG. 8. Time change of salinity in grids on the S-line (Fig. 7a), which is necessary for the production of the low-salinity water mass. Letters a, b, c and d correspond to those on the S-line in Fig. 7a.

advanced time backward from 10 August. A time series of the location of the particles is given in Fig. 10. Figure 10 shows that the particles in the southern half of the low-salinity water on the Kuroshio, especially the particles having a ΔS value larger than 0.4‰ and denoted by the solid squares and crosses, moved quite close to the coast of Kyushu and Shikoku and they could be expected to receive a large amount of fresh water discharged from the Bungo Channel, the Tosa Bay and the Kii Channel. On the other hand, particles in the northern half of the low-salinity water seemed to be trapped for a long time inside the anticlockwise circulation adjacent to the Kuroshio.
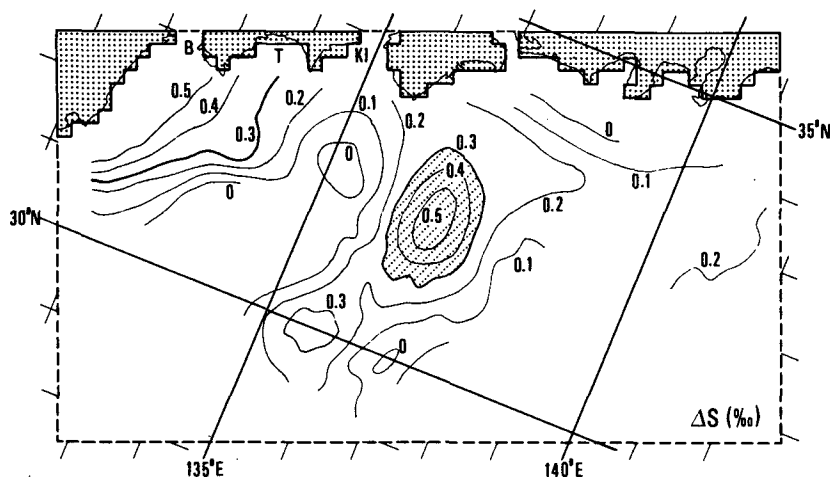
FIG. 9. Distribution of salinity difference (ΔS) between the measured salinity (Fig. 3d) and the salinity distribution deduced from theoretical particle tracking (Fig. 7f). B, T and KI: the same as in Fig. 1.

To determine whether the supply of fresh water from the coast is sufficient to make the low-salinity water mass, we roughly estimated the volume of fresh water required to form it by the following method. We considered a situation in which we dilute a saline water of volume W and salinity S_1‰ to obtain water of salinity S‰ by adding a volume F of water of salinity S_0‰. Balancing volume and salt, we find that F is given by

$$F = \frac{S_1 - S}{S_1 - S_0} T,$$

where T is the total ($W + F$) water volume. We set $S_0 = 0$, because a supply of fresh water is assumed. To estimate the total water volume (T), we used the observed vertical profile of salinity across the low-salinity water mass (Fig. 3e) and the patterns of similarity between the observed surface salinity distribution (Fig. 3d) and the calculated ΔS ($=S_1 - S$) distribution (Fig. 9) in the neighborhood of the low-salinity water mass. As a result, the volume of fresh water (F) required to dilute the water mass for which ΔS is larger than 0.3‰ is then evaluated to be 3.9×10^9 tons.

c. Volume of river water discharge

In this section, we examine whether there were such excessive discharges from the coast. Figure 11 shows the discharge variations in 1979 for the rivers Yodo, Yoshino and Oyodo, which are the representative large rivers in southern Japan. In this figure, solid arrowheads show the date of observation of the low-salinity water; i.e., 10 August 1979. We found that a dominant peak of river water discharge appeared during June 29–July 3, about 40 days before the observation, and that the peak value exceeded ten times the annual-mean discharge, which is shown in the figure by a broken line. The tendency of such an excessive water discharge appeared in almost all the large rivers in southern Japan. In Table 1, we tabulated the discharged volumes for the three groups of large rivers which flow into the Kii Channel, the Tosa Bay and the Bungo Channel. The position of the rivers in these three groups is shown by the inverted triangle, ∇ and solid triangle, respectively, in Fig. 12. The total water volume discharged over the heavy rainfall period from 29 June to 3 July was 6.7×10^9 tons. Consequently, if the low-salinity water mass was produced by the excessive river-water discharge, about 58% of the discharge was sufficient to form the low-salinity water mass.

d. Effect of precipitation

Another possible source of fresh water to form the low-salinity water mass could be rain water falling directly on the group of water particles in the low-salinity water mass (Fig. 10). To evaluate the amount of rain water supply, we used radar-echo pictures taken at Cape Muroto by the Muroto Meteorological Observatory at time intervals of 1–3 hours from 19 July to 10 August 1979. Figure 13a shows an example of the radar-echo picture taken at 9:00 a.m. on 6 August 1979. Figure 13b shows the distribution of the particles for 6 August which is the same as in Fig. 10f, and the broken line in Fig. 13a denotes the boundary of the cluster of particles shown in Fig. 13b. In the radar-echo picture, precipitation is classified in three ranks: 0–4, 4–16 and larger than 16 mm h^{-1}. Therefore, we evaluated the total volume of rain water by

$$\sum_k \left\{ \sum_i P_i S_i \right\} \Delta t_k,$$

where precipitation P_i is taken as $P_1 = 2$, $P_2 = 10$ and $P_3 = 20$ mm h^{-1}, S_i is the area of P_i, and Δt_k is the time interval at which the radar-echo pictures were
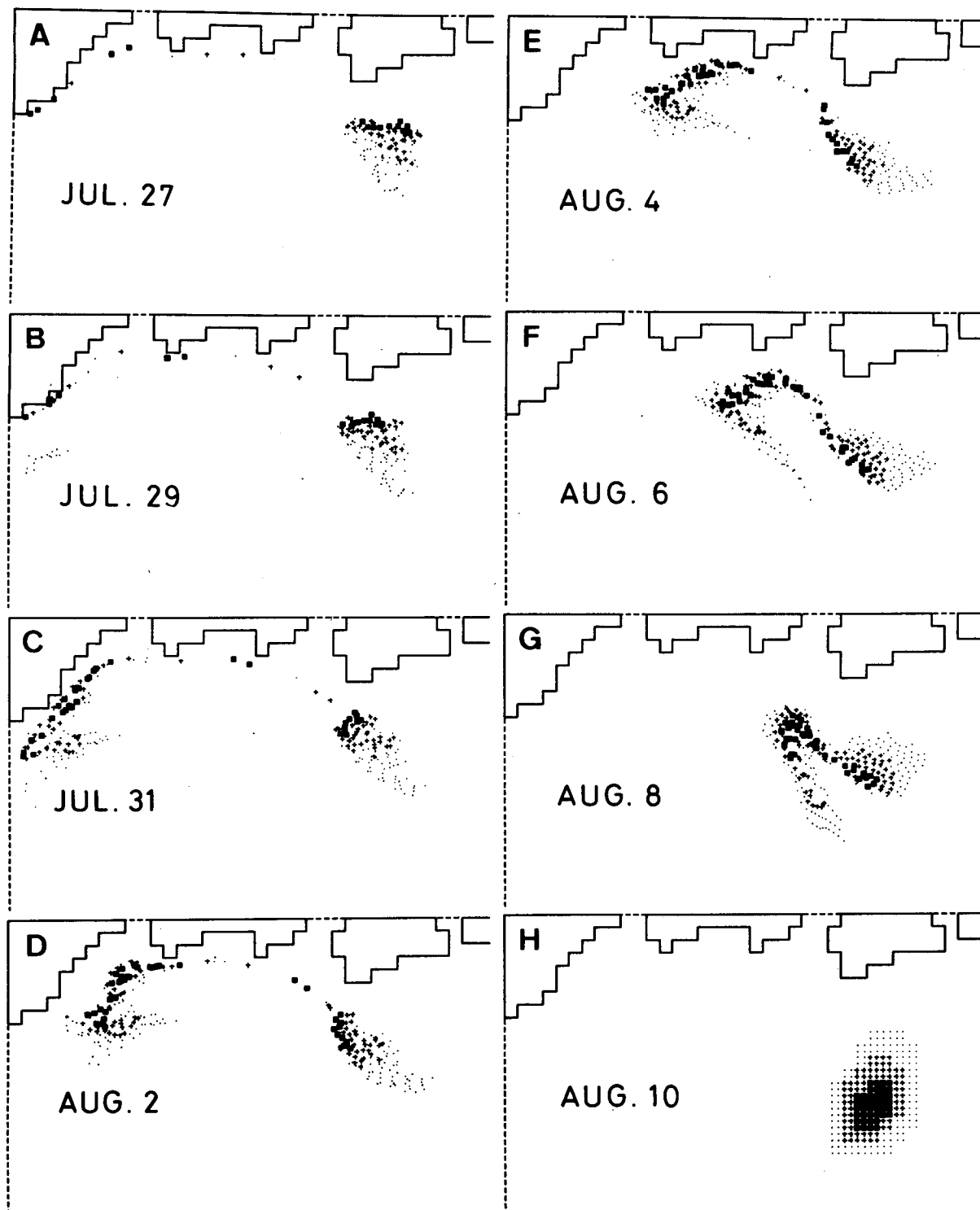
FIG. 10. Trajectory of the particles in the low-salinity water mass. Solid squares, crosses and solid circles denote a water particle with $\Delta S > 0.5\%o$, $\Delta S = 0.4 \sim 0.5\%o$ and $\Delta S = 0.3 \sim 0.4\%o$, respectively.

taken. The estimation was done by putting the radar-echo picture over the corresponding panel of particle distribution; e.g., Figure 13a is put over Fig. 10f, and

the k values from 1200 20 July to 1200 10 August 1979 were summed. The results show that the particles in the low-salinity water mass obtained 4.1×10^8 tons of
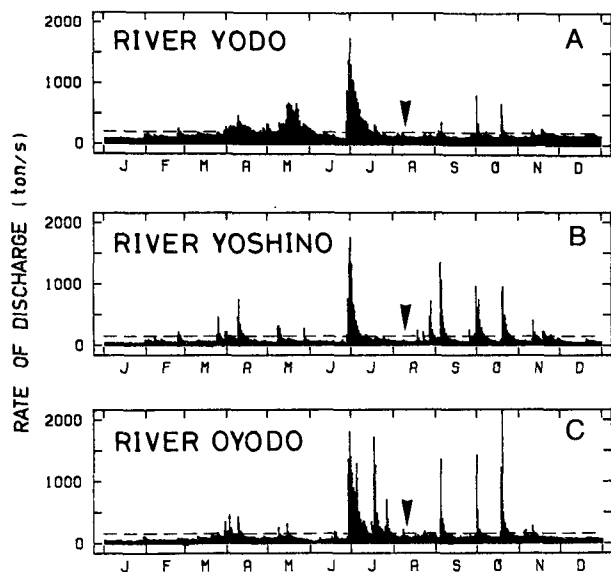
FIG. 11. Time variations of river water discharge in 1979 for the Yodo, the Yoshino and the Oyodo rivers. The broken line denotes the annual mean discharge for each river. An arrowhead indicates the date of the observation of the low-salinity water mass.

fresh water originating from the precipitation, which is only about 10% of the required F. Thus, we could neglect the effect of the direct supply of fresh water due to precipitation in forming the low-salinity water mass

on the Kuroshio. However, if we take into account the direct supply of rain water, about 52% of the river water discharge would be sufficient to produce the low-salinity mass.

e. The possibility of a particle in the low-salinity water mass encountering a parcel of discharged fresh water

Having excluded the possibility of direct supply of rain water as the major source of the low-salinity water on the Kuroshio, we examined whether a particle in the low-salinity water mass could encounter a parcel of fresh water discharged from the Seto-Inland Sea or the Tosa Bay while moving across the continental shelf of southern Japan. Now we consider the situation in which a fresh water parcel was discharged from a major river in southern Japan on 29 June 1979, the first day of the discharge peak, and moved through the coastal region to the continental shelf region at a constant speed. Figure 14 shows the relationship between the speed of the fresh water parcel and the date when the parcel arrives at line C (Fig. 12), which is a representative boundary between the Kuroshio and the shelf water; e.g., the isoline of salinity of 34‰ in Fig. 2. In this figure, we plotted the relationship for the 16 major rivers with a discharge rate exceeding 500 ton s^{-1} during the period of heavy discharge. The numbers of the major rivers are keyed to Table 1.

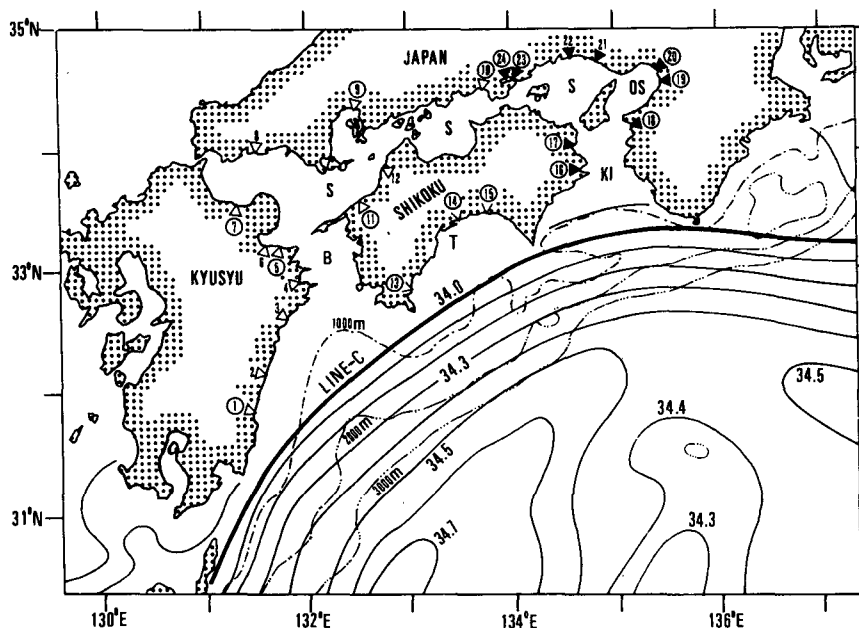As already shown in Fig. 10, the southern half of the

FIG. 12. Position of river mouths. Numbers correspond to the river names in Table 1. Rivers with discharge rate exceeding 500 ton s^{-1} are indicated by circled numbers. Inverted triangles, ∨ and solid triangles denote the rivers from which water moves towards the Bungo Channel, the Tosa Bay and the Kii Channel, respectively. S, B, T and KI: the same as in Fig. 1, and OS: the Osaka Bay. Line-C is a representative boundary between the Kuroshio and the shelf water.

TABLE 1. Rate of discharge (ton s⁻¹) of major rivers from which water moves towards the Bungo Channel, the Tosa Bay and the Kii Channel. "Event-mean" denotes the rate of discharge averaged over five days from 29 June to 3 July 1979.

Section	Number	River names	Event-mean	Annual-mean
Bungo	1	Oyodo	1320.9	160.7
Channel	2	Omaru	302.2	38.4
	3	Gokase	421.4	64.6
	4	Bansho	114.4	15.4
	5	Ono	510.3	62.5
	6	Oita	305.8	29.8
	7	Yamakuni	563.6	27.3
	8	Saba	295.6	20.5
	9	Ota	676.8	83.2
	10	Takahashi	649.3	62.7
	11	Hiji	681.0	44.7
	12	Shigenobu	305.2	14.9
Total			6399.5	624.7
Tosa	13	Shimanto	1333.4	135.8
Bay	14	Niyodo	964.0	124.9
	15	Monobe	587.0	39.9
Total			2884.3	300.6
Kii	16	Naka	544.1	81.5
Channel	17	Yoshino	1210.7	149.5
	18	Kino	606.2	53.1
	19	Yamato	553.3	28.7
	20	Yodo	1293.2	206.4
	21	Kako	366.3	43.8
	22	Ibo	272.8	21.8
	23	Yoshii	689.5	75.5
	24	Asahi	585.1	59.0
Total			6130.2	719.3

particles in the low-salinity water mass passed the off-shore region of the Bungo Channel, the Tosa Bay and the Kii Channel between 20 July and 8 August. In order for the fresh water parcels discharged from the rivers to encounter the cluster of particles of the low-salinity water mass, they had to arrive at the vicinity of line C between 20 July and 8 August 1979. This period is shown by the shaded area in Fig. 14. A water parcel, for example, discharged on 29 June from the Yodo River (Number 20 in Fig. 12), must move at a constant speed of 6–10 cm s⁻¹ to encounter the particles of the low-salinity water mass on the continental shelf region during the critical period. From Fig. 14, we concluded that the low-salinity water mass could be produced on the Kuroshio if fresh water parcels discharged from the rivers moved through the coastal areas with a mean speed of about 5–10 cm s⁻¹. Using an ultrasonic current meter fixed to an observation tower in the Osaka Bay (135°14.4′E, 34°25.8′N), Murakami et al. (1982) measured the current velocity for a period of four years and obtained an annual mean speed of 3–7 cm s⁻¹ at 9 m below the average sea surface. They

also found that the annual mean speed was proportional to the river water discharge. Their annual mean speed agrees with our estimated mean speed, which seems to be a reasonable speed for a density current in a coastal region.

4. Discussion and conclusion

In this study, we used field observational data and the Euler–Lagrangian method to determine the origin of the low-salinity water masses encountered on the Kuroshio from 1967 to 1981. The Euler–Lagrangian method was used by Imasato et al. (1980) and Awaji et al. (1980) to study the tidal exchange through a narrow strait. Based on this method, we numerically tracked particles in the representative low-salinity water mass encountered on 10 August 1979.

In the present examination, however, we have some ambiguities: the first is the fact that the distributions of Eulerian velocity and salinity are based on some cruises of serial observation which were performed during a three-month period. It would have been better to have more synoptic observations, such as from a satellite. The second is the assumption that the velocity field is in geostrophic balance. Because the nonlinear effect of the meandering Kuroshio may not be neglected and the velocity at coastal and shelf regions may deviate considerably from geostrophic balance, we need to establish a more reliable method of estimating diagnostically the Eulerian velocity field from observations of temperature and salinity in the sea, including shallow areas.

The formation of the low-salinity water masses on the Kuroshio must be affected by additional factors which we have not mentioned, such as wind stress, evaporation and mixing processes. Our feeling is that if these factors were included, the results would not alter significantly. If we want to take them into account, however, we must evaluate all these physical elements as functions of space and time at the position of each particle, in the way that we used radar-echo pictures in evaluating the precipitation. Unfortunately, we have no time series of wind speed, vapor pressure, air temperature, or water temperature at the sea surface. Mixing processes will be induced by the interaction between the Kuroshio and the wave motions such as tidal currents or wind waves, and by vertical convection produced by sea surface cooling. The mixing processes could be taken into account by adding a turbulent velocity generated in a computer by Gaussian random numbers to the Lagrangian velocity of each particle, but we have not performed this procedure because of uncertainties in the formula and magnitude for the diffusivity. In this study we believe it more likely that the cause of the low-salinity water mass is fresh water from Japanese rivers emptying into the coastal region, but it *is* possible that the observed effect could be due
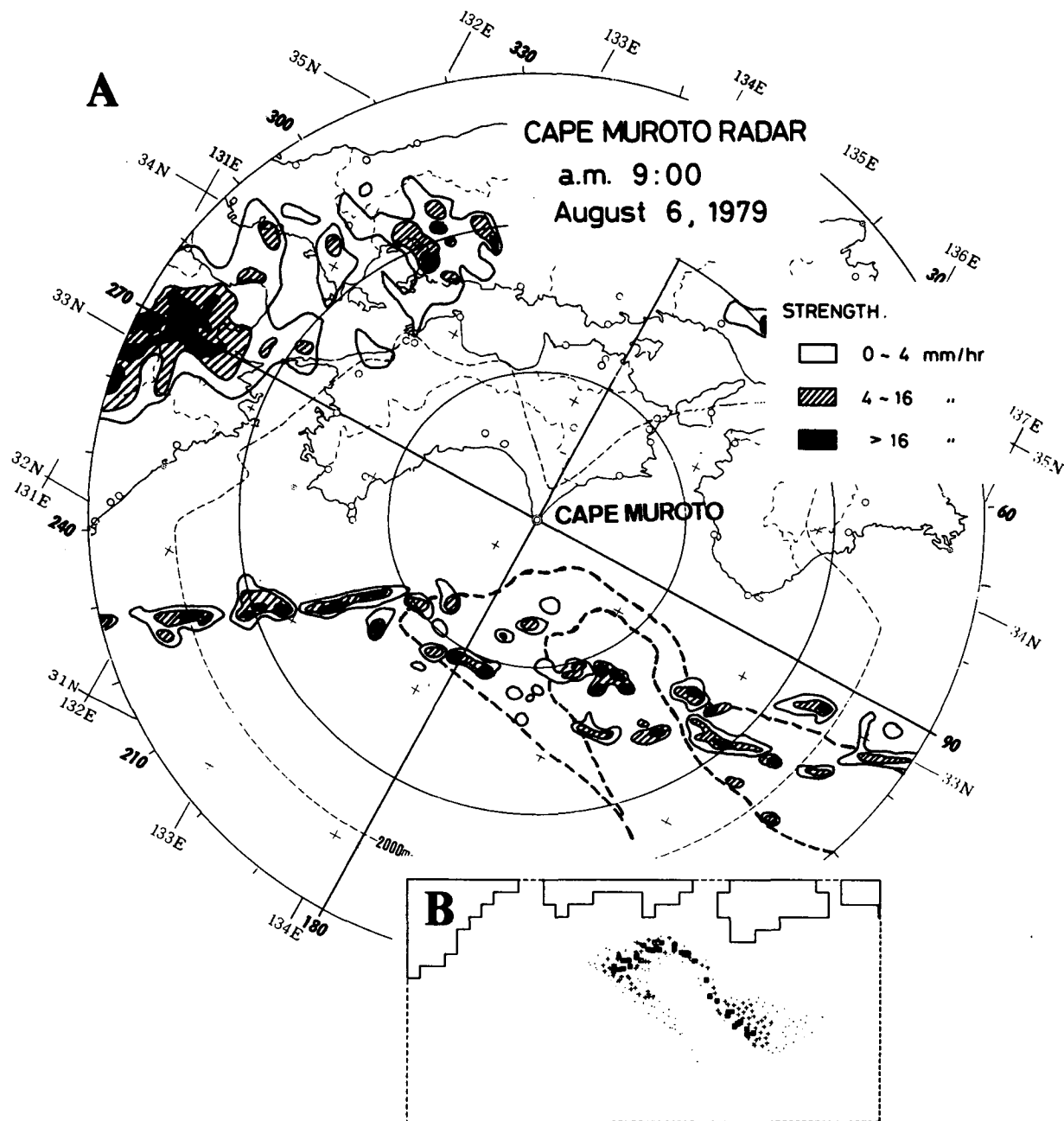
Fig. 13. An example of a radar-echo picture taken at Cape Muroto by the Muroto Meteorological Observatory. (a) a sketch of the radar-echo observed at 9:00 a.m. 6 August 1979. (b) theoretical distribution of particle cluster predicted at the same time as panel A (the same figure as Fig. 10f).

to low salinity water moving into the East China Sea and from the shelf region east of the Kii Peninsula. However, these problems have been left for future studies.

Our conclusions in this study are as follows:

1) Large low-salinity water masses emerge on the Kuroshio offshore of Japan only in spring and summer. Many of them are accompanied by a heavy discharge of fresh water from the major rivers in southern Japan. These discharges are much larger than the annual mean value of discharge and are probably produced by snow melting in spring and by rain fall due to a stagnating front, a cyclone or a typhoon. The low-salinity water masses were mainly observed 20–40 days after the heavy discharge had occurred.
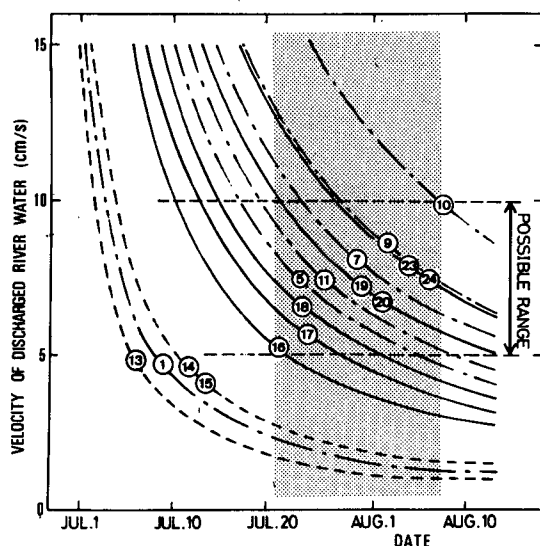
FIG. 14. Estimation of possible speed for a parcel of discharged river water moving in the coastal area. Numbers in the circle correspond to the river names in Table 1.

2) The salinity difference ΔS between the low-salinity water mass and the Kuroshio is closely proportional to the volume of the discharged river water.

3) The low-salinity water mass observed on 10 August 1979 was examined to determine the origin of fresh water by the numerical method of Euler–Lagrange. The following results were obtained:

(i) This low-salinity water mass was produced by fresh waters discharged from the major rivers in southern Japan due to a heavy rain fall, moved towards the shelf off the Bungo and the Kii channels and the Tosa Bay and intruded into the Kuroshio.

(ii) If the fresh water supplied to the low-salinity water mass originated from the Seto-Inland Sea and the Tosa Bay, we estimate the 58% of the volume of river water discharged from the major rivers during 29 June to 3 July 1979 forms the low-salinity water mass.

(iii) The effect of precipitation on producing the low-salinity water mass on the Kuroshio can be neglected. However, if we take into account the direct supply of rain water, 52% of the volume of river water discharge would be sufficient to produce the low-salinity water mass.

(iv) A parcel of fresh water is estimated to move through the coastal areas as a density current from a river mouth to the continental shelf at a mean speed of 5–10 cm s^{-1}.

REFERENCES

Awaji, T., N. Imasato and H. Kunishi, 1980: Tidal exchange through a strait: A numerical experiment using a simple model basin. *J. Phys. Oceanogr.,* **10,** 1499–1508.

Fisher, A., Jr., 1972: Entrainment of shelf water by the Gulf Stream northeast of Cape Hatteras. *J. Geophys. Res.,* **77,** 3248–3255.

Ford, W. L., and N. Miller (1952): The surface layer of the Gulf Stream and adjacent waters. *J. Mar. Res.,* **11,** 267–280.

——, J. R. Longard and R. E. Banks, (1952): On the nature, occurence and origin of cold low-salinity water along the edge of the Gulf Stream. *J. Mar. Res.,* **11,** 281–293.

Fuglister, F. C. (1972): Cyclonic rings formed by the Gulf Stream: 1965–1966. *Studies in Physical Oceanography, Vol. 1,* Gordon and Breach, 137–167.

Horne, E. P. W. (1978): Interleaving at the subsurface front in the Slope water off Nova Scotia. *J. Geophys. Res.,* **83,** 3659–3671.

Imasato, N., T. Awaji and H. Kunishi (1980): Tidal exchange through Naruto, Akashi and Kitan Straits. *J. Oceanogr. Soc. Japan,* **36**(3), 151–162.

Kawabe, M. (1985): Sea level variations at the Izu Islands and typical stable paths of the Kuroshio. *J. Oceanogr. Soc. Japan,* **41**(5), 307–326.

Kawai, H. (1969): Statistical estimation of isotherms indicatives of the Kuroshio Axis. *Deep-Sea Res.,* **16,** 109–115.

Kupferman, S. L., and N. Garfield (1977): Transport of low-salinity water as the Slope Water-Gulf Stream boundary. *J. Geophys. Res.,* **82,** 3481–3486.

Kuroda, K. (1969): Short-term variations of the surface diatoms in the Kuroshio. *Oceanogr. Mag.,* **21,** 97–111.

Lambert, R. B., Jr. (1982): Lateral mixing processes in the Gulf Stream. *J. Phys. Oceanogr.,* **12,** 851–861.

Lee, T. N., L. P. Atkinson and R. Legeckis (1981): Observations of a Gulf Stream frontal eddy on the Georgia continental shelf, April 1977. *Deep-Sea Res.,* **28,** 347–378.

Murakami, K., M. Morikawa and T. Sakaguchi (1982): Wind effect and water discharge effect on constant flow: Discussion using observation data at Off-Sennan (1978–1981). *Rep., Port Harbour Res. Inst.,* **21**(4), 3–39 (in Japanese).

Saunders, P. M. (1971): Anticyclonic eddys formed from shoreward meanders of the Gulf Stream. *Deep-Sea Res.,* **18,** 1207–1219.

Takano, I., S. Imawaki and H. Kunishi (1981): Surface temperature-salinity front in the Kuroshio south of Japan. *La mer,* **19,** 171–178.